A&A, 690, C2 (2024)
https://doi.org/10.1051/0004-6361/202451843e

Astronomy & Astrophysics

Letter to the Editor

The dispersion of the $E_{p,i}$–L_{iso} correlation of long gamma-ray bursts is partially due to assembling different sources (*Corrigendum*)

M. Maistrello[1,⋆], R. Maccary[1], C. Guidorzi[1,2,3], and L. Amati[3]

[1] Department of Physics and Earth Science, University of Ferrara, Via Saragat 1, I-44122 Ferrara, Italy
[2] INFN – Sezione di Ferrara, Via Saragat 1, 44122 Ferrara, Italy
[3] INAF – Osservatorio di Astrofisica e Scienza dello Spazio di Bologna, Via Piero Gobetti 101, 40129 Bologna, Italy

A&A, 684, L10 (2024), https://doi.org/10.1051/0004-6361/202449165

Key words. methods: data analysis – methods: statistical – gamma-ray burst: general – errata, addenda

We found a mistake in the code used to compute the parameters m, q, and σ_{int} of the $E_{p,i}$–L_{iso} and $E_{p,i}$–L_{coll} correlations reported in Tables 1, 2, and 3. We verified to see whether the essence of our results remains unaffected, and in fact the statistical evidence of our conclusions is even stronger than what was reported in the Letter.

For each burst in the sample, we recomputed the aforementioned parameters and provide the correct values in Tables 1, 2, and 3, which are meant to replace those reported in the Letter. We also provide the amended version of Fig. 1. Not only do the general conclusions that we found remain valid, but the main result shown in Sect. 3.1 improved. In fact, with reference to that section, the statistical significance goes from 4.2 ($P_t = 2.69 \times 10^{-5}$) to 5.9$\sigma$ (Gaussian, $P_t = 4.55 \times 10^{-9}$).

Referring to Sect. 3.3, we provide here the correct values of the parameters of GRB 090102: $m_B = 0.82^{+0.33}_{-0.32}$, $q_B = 2.46^{+0.18}_{-0.20}$, and $\sigma_{int,B} = 0.24^{+0.17}_{-0.08}$.

References

Camisasca, A. E., Guidorzi, C., Amati, L., et al. 2023, A&A, 671, A112
Chand, V., Chattopadhyay, T., Oganesyan, G., et al. 2019, ApJ, 874, 70
Ghirlanda, G., Nappo, F., Ghisellini, G., et al. 2018, A&A, 609, A112
Zhao, W., Zhang, J.-C., Zhang, Q.-X., et al. 2020, ApJ, 900, 112
Zhu, Z.-P., Lei, W.-H., Malesani, D. B., et al. 2023, ApJ, 959, 118

⋆ Corresponding author; mstmnl@unife.it

Table 1. Sample of GRBs with redshift z, jet half-opening angle θ_j – both in the homogeneous interstellar medium (ISM) and wind profile (W) –, the Lorentz factor Γ_0, and the minimum variability timescale (MVT).

GRB	z	$\theta_j^{(ISM)}$ (10^{-2} rad)	$\theta_j^{(W)}$ (10^{-2} rad)	Γ_0	MVT (s)	m	q	σ_{int}	N	$(\log(E_{p,i}/\mathrm{keV}))_c$
090102	1.547	n.a.	n.a.	215^{+11}_{-10}	$0.123^{+0.043}_{-0.032}$	$0.86^{+0.17}_{-0.17}$	$2.38^{+0.09}_{-0.09}$	$0.19^{+0.08}_{-0.05}$	18	2.52 ± 0.08
090323	3.5832	10.3 ± 4.3	4.5 ± 1.2	489^{+30}_{-30}	$0.465^{+0.161}_{-0.120}$	$0.54^{+0.23}_{-0.21}$	$2.50^{+0.25}_{-0.26}$	$0.27^{+0.08}_{-0.06}$	32	2.59 ± 0.21
090328	0.736	n.a.	n.a.	141^{+15}_{-11}	$0.189^{+0.065}_{-0.049}$	$0.65^{+0.14}_{-0.15}$	$2.96^{+0.09}_{-0.09}$	$0.19^{+0.07}_{-0.05}$	24	3.07 ± 0.11
090424	0.544	<23.1	<16.1	300^{+79}_{-79}	$0.073^{+0.025}_{-0.019}$	$0.44^{+0.05}_{-0.05}$	$2.19^{+0.03}_{-0.03}$	$0.10^{+0.03}_{-0.02}$	34	2.27 ± 0.03
091208B	1.0633	<14.8	<13.8	500^{+33}_{-33}	$0.092^{+0.032}_{-0.024}$	$0.46^{+0.07}_{-0.07}$	$2.24^{+0.03}_{-0.04}$	$0.04^{+0.05}_{-0.03}$	13	2.32 ± 0.05
100414A	1.368	n.a.	n.a.	262^{+8}_{-7}	$0.105^{+0.036}_{-0.027}$	$0.87^{+0.37}_{-0.36}$	$2.43^{+0.29}_{-0.30}$	$0.22^{+0.10}_{-0.06}$	16	2.58 ± 0.24
100728A	1.567	n.a.	n.a.	250^{+9}_{-8}	$0.101^{+0.035}_{-0.026}$	$0.45^{+0.08}_{-0.09}$	$2.69^{+0.04}_{-0.03}$	$0.12^{+0.03}_{-0.02}$	46	2.77 ± 0.03
100906A	1.727	2.9 ± 0.1	3.0 ± 0.1	<369	$0.917^{+0.317}_{-0.236}$	$0.74^{+0.17}_{-0.18}$	$2.20^{+0.09}_{-0.08}$	$0.16^{+0.09}_{-0.06}$	9	2.32 ± 0.08
120711A	1.405	n.a.	n.a.	250^{+7}_{-7}	$0.083^{+0.029}_{-0.021}$	$0.62^{+0.11}_{-0.11}$	$2.61^{+0.10}_{-0.09}$	$0.12^{+0.05}_{-0.04}$	27	2.72 ± 0.08
140508A	1.027	n.a.	n.a.	500^{+17}_{-16}	$1.044^{+0.361}_{-0.268}$	$0.61^{+0.11}_{-0.12}$	$2.40^{+0.07}_{-0.07}$	$0.24^{+0.07}_{-0.05}$	32	2.51 ± 0.08
140512A	0.725	4.7 ± 0.1	5.2 ± 0.1	92^{+11}_{-8}	$0.434^{+0.150}_{-0.112}$	$0.46^{+0.10}_{-0.11}$	$2.90^{+0.09}_{-0.09}$	$0.11^{+0.05}_{-0.04}$	21	2.98 ± 0.12
151027A	0.81	7.9 ± 0.9	8.3 ± 0.6	143^{+20}_{-17}	$1.845^{+0.638}_{-0.474}$	$0.57^{+0.28}_{-0.27}$	$2.72^{+0.28}_{-0.27}$	$0.28^{+0.14}_{-0.08}$	15	2.82 ± 0.32
160509A	1.17	9.2 ± 0.7	5.4 ± 0.3	470^{+22}_{-21}	$0.515^{+0.178}_{-0.132}$	$0.27^{+0.06}_{-0.06}$	$2.58^{+0.05}_{-0.04}$	$0.15^{+0.03}_{-0.03}$	50	2.63 ± 0.04
160625B	1.406	14.8 ± 1.0	6.0 ± 0.3	860^{+19}_{-19}	$0.174^{+0.060}_{-0.045}$	$0.38^{+0.05}_{-0.05}$	$2.46^{+0.08}_{-0.07}$	$0.16^{+0.03}_{-0.02}$	73	2.53 ± 0.06
170405A	3.510	2.0 ± 0.1	2.8 ± 0.1	n.a.	$0.605^{+0.209}_{-0.155}$	$0.33^{+0.16}_{-0.17}$	$2.70^{+0.20}_{-0.20}$	$0.13^{+0.06}_{-0.04}$	23	2.76 ± 0.16
171010A [(a)]	0.3285	<11.0	n.a.	201^{+7}_{-7}	$0.364^{+0.126}_{-0.094}$	$0.40^{+0.05}_{-0.05}$	$2.39^{+0.04}_{-0.04}$	$0.19^{+0.02}_{-0.02}$	162	2.46 ± 0.05
180720B	0.654	7.2 ± 0.7	5.3 ± 0.3	n.a.	$0.090^{+0.031}_{-0.023}$	$0.36^{+0.06}_{-0.06}$	$2.60^{+0.04}_{-0.04}$	$0.18^{+0.03}_{-0.02}$	93	2.66 ± 0.03
181020A	2.938	2.1 ± 0.3	2.0 ± 0.2	n.a.	$0.376^{+0.130}_{-0.097}$	$0.39^{+0.18}_{-0.18}$	$2.58^{+0.23}_{-0.24}$	$0.11^{+0.09}_{-0.04}$	10	2.66 ± 0.21
190114C	0.4245	3.2 ± 0.5	3.2 ± 0.3	n.a.	$0.098^{+0.034}_{-0.025}$	$0.61^{+0.04}_{-0.04}$	$2.43^{+0.04}_{-0.04}$	$0.20^{+0.04}_{-0.03}$	64	2.53 ± 0.04
221010A [(b)]	4.615	6^{+1}_{-2}	n.a.	n.a.	n.a.	$0.40^{+0.09}_{-0.10}$	$2.48^{+0.13}_{-0.12}$	$0.12^{+0.04}_{-0.03}$	31	2.56 ± 0.10

Notes. Values of z and θ_j are from Zhao et al. (2020), Γ_0 from Ghirlanda et al. (2018), and MVT from Camisasca et al. (2023). Also reported are the best-fit parameters of the $E_{p,i}$–L_{iso} correlation (90% confidence), the number of spectra N, and the representative value of $\log E_{p,i}$ computed at a common reference luminosity (see Sect 3.2). [(a)] $\theta_j^{(ISM)}$ is taken from Chand et al. (2019). [(b)] z and $\theta_j^{(ISM)}$ are taken from Zhu et al. (2023).

Table 2. Best-fit parameters of the $E_{p,i}$–L correlation (90% confidence) for the overall sample $\mathcal{S}$ and for the sub-samples $\mathcal{S}^{(ISM)}$ and $\mathcal{S}^{(W)}$ of time-resolved spectra of GRBs with available information on $\theta_j^{(ISM)}$ and on $\theta_j^{(W)}$, respectively.

	Set	N_{int}	N_{GRB}	m_t	q_t	$\sigma_{int,t}$
$E_{p,i}$–L_{iso}	$\mathcal{S}$	793	20	$0.46^{+0.02}_{-0.02}$	$2.50^{+0.02}_{-0.02}$	$0.24^{+0.01}_{-0.01}$
$E_{p,i}$–L_{iso}	$\mathcal{S}^{(ISM)}$	421	11	$0.41^{+0.02}_{-0.02}$	$2.54^{+0.02}_{-0.02}$	$0.23^{+0.01}_{-0.01}$
$E_{p,i}$–L_{iso}	$\mathcal{S}^{(W)}$	390	10	$0.41^{+0.02}_{-0.02}$	$2.53^{+0.02}_{-0.02}$	$0.24^{+0.02}_{-0.01}$
				$\bar{m} \pm \sigma_m$	$\bar{q} \pm \sigma_q$	$\bar{\sigma}_{int} \pm \sigma_\sigma$
$E_{p,i}$–L_{iso}	$\mathcal{S}$	793	20	0.52 ± 0.17	2.52 ± 0.21	0.16 ± 0.06
				m_{coll}	q_{coll}	σ_{coll}
$E_{p,i}$–$L_{coll}^{(ISM)}$	$\mathcal{S}^{(ISM)}$	421	11	$0.29^{+0.02}_{-0.02}$	$3.34^{+0.05}_{-0.05}$	$0.29^{+0.02}_{-0.02}$
$E_{p,i}$–$L_{coll}^{(W)}$	$\mathcal{S}^{(W)}$	390	10	$0.38^{+0.02}_{-0.02}$	$3.68^{+0.06}_{-0.06}$	$0.25^{+0.02}_{-0.02}$

Notes. We note that N_{int} and N_{GRB} are the total number of intervals and the number of GRBs, respectively, while $\bar{m} \pm \sigma_m$, $\bar{q} \pm \sigma_q$, and $\bar{\sigma}_{int} \pm \sigma_\sigma$ are the mean values and standard deviations of the distributions of the best-fit parameters of the individual GRBs reported in Table 1. The luminosity is either isotropic-equivalent (iso) or collimation-corrected (coll).

Table 3. Best-fit parameters of the $E_{p,i}$–L_{iso} correlation (90% confidence) of the GRBs with the highest S/N obtained including BGO data with a better viewing angle (m_{BGO}, q_{BGO}, and $\sigma_{int,BGO}$ using the Band function; m_{CPL}, q_{CPL}, and $\sigma_{int,CPL}$ using the CPL model) and NaI alone (m, q, and σ_{int}).

GRB	m_{BGO}	q_{BGO}	$\sigma_{int,BGO}$	N_β/N_{BGO}
160625B	$0.37^{+0.06}_{-0.06}$	$2.56^{+0.10}_{-0.09}$	$0.17^{+0.03}_{-0.03}$	33/72
171010A	$0.46^{+0.06}_{-0.06}$	$2.47^{+0.04}_{-0.04}$	$0.18^{+0.02}_{-0.02}$	64/159
180720A	$0.35^{+0.07}_{-0.07}$	$2.71^{+0.04}_{-0.04}$	$0.17^{+0.03}_{-0.02}$	10/86
GRB	m_{CPL}	q_{CPL}	$\sigma_{int,CPL}$	
160625B	$0.39^{+0.07}_{-0.07}$	$2.65^{+0.11}_{-0.10}$	$0.20^{+0.04}_{-0.03}$	
171010A	$0.45^{+0.05}_{-0.05}$	$2.61^{+0.04}_{-0.04}$	$0.17^{+0.02}_{-0.02}$	
180720A	$0.40^{+0.07}_{-0.07}$	$2.82^{+0.04}_{-0.04}$	$0.17^{+0.03}_{-0.02}$	
GRB	m	q	σ_{int}	
160625B	$0.38^{+0.05}_{-0.05}$	$2.46^{+0.08}_{-0.07}$	$0.16^{+0.03}_{-0.02}$	
171010A	$0.40^{+0.05}_{-0.05}$	$2.39^{+0.03}_{-0.03}$	$0.19^{+0.02}_{-0.02}$	
180720A	$0.36^{+0.06}_{-0.06}$	$2.60^{+0.04}_{-0.04}$	$0.18^{+0.03}_{-0.02}$	

Notes. We note that N_{BGO} and N_β are the number of selected intervals and those with an estimated β including BGO data, respectively.

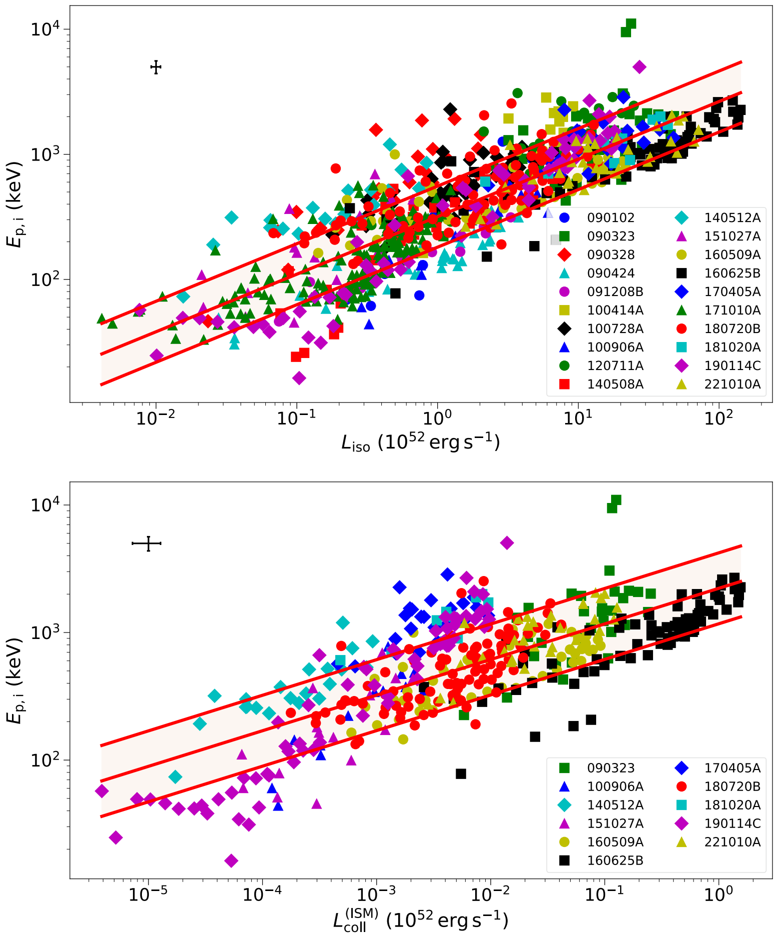

Fig. 1. Top panel: Time-resolved $E_{p,i}$–L_{iso} relation for the overall sample $\mathcal{S}$. Bottom panel: Collimation-corrected $E_{p,i}$–L_{coll} relation for the subset $\mathcal{S}^{(ISM)}$ of GRBs with available information on $\theta_j^{(ISM)}$. In both panels the best-fit model along with the 1-$\sigma_{int,t}$ region (shaded area) is shown, while median uncertainties along both axes are shown in the top left.